Available online at www.sciencedirect.com

ScienceDirect

Procedia IUTAM 13 (2015) 71 – 81

Procedia IUTAM

www.elsevier.com/locate/procedia

IUTAM Symposium on "Dynamical Analysis of Multibody Systems with Design Uncertainties"

Analysis of Design Uncertainties in Structurally Optimized Lightweight Machines

Robert Seifried*, Ali Moghadasi, Alexander Held

Institute of Mechanics and Ocean Engineering, Hamburg University of Technology, 21071 Hamburg, Germany

Abstract

Structural optimization methods have been recently successfully applied in optimizing dynamical systems and lightweight machines. The main goal is to reduce the mass of flexible members without deteriorating the accuracy of the system. In this paper, structural optimization based on topology optimization of members of flexible multibody system is introduced and the effects of uncertainty in the optimization process are investigated. Two sources of uncertainty, namely the model uncertainty and the uncertainty in usage are addressed. As an application example, a two-arm manipulator is used to examine and illustrate the effects of uncertainties such as different objective functions, choices of model reduction method as well as changes in the trajectory and payload of the manipulator.

© 2015 The Authors. Published by Elsevier B.V. This is an open access article under the CC BY-NC-ND license (http://creativecommons.org/licenses/by-nc-nd/4.0/).
Peer-review under responsibility of organizing committee of Institute of Engineering and Computational Mechanics University of Stuttgart.

Keywords: design uncertainty; lightweight design; multibody system; topology optimization

1. Introduction

Energy efficiency is a permanent issue in machine design, such as industrial robots or machine tools. In order to reduce the energy consumption, lightweight design techniques are applied to lower the moving masses and to improve the mass to payload ratio. However, as a result, the stiffness of the bodies decreases and non-negligible structural deformations might appear during the working motion. For example in lightweight manipulators, structural flexibility might lead to large unacceptable end-effector tracking errors. Thus, these deformations are a point of concern especially for high speed and high precision machines. To decrease tracking errors one could use modern nonlinear control approaches[4]. However, implementing these control approaches on standard machine hardware might be challenging. Alternatively, it is possible to employ structural optimization methods and stiffen the members of the flexible system with regard to the dynamical loads they are exposed to. The present research analyses structural optimization methods, more precisely topology optimization, with a special concern for the influence of design and application uncertainties.

* Corresponding author. Tel.: +49-(0)40-42878-3020 ; fax: +49-(0)40-42878-2028.
E-mail address: robert.seifried@tuhh.de

2210-9838 © 2015 The Authors. Published by Elsevier B.V. This is an open access article under the CC BY-NC-ND license (http://creativecommons.org/licenses/by-nc-nd/4.0/).
Peer-review under responsibility of organizing committee of Institute of Engineering and Computational Mechanics University of Stuttgart.
doi:10.1016/j.piutam.2015.01.018

In the structural optimization, objective functions are often formulated with regard to the results of time simulations of the flexible multibody system. In this way, the actual dynamic loads can be taken into account and the tracking behavior of the total multibody system can be directly improved. First promising results of such optimization strategies are discussed in [1,2,3,5] for various types of active flexible multibody systems.

In this paper, for the optimal system design, the objective functions are computed from fully dynamical simulations of a flexible multibody system, which is modeled using the floating frame of reference formulation [21]. Thereby, employing the equivalent static load method [17], the relevant loads, which act during the motion on the flexible members of the system, are captured. Consequently, all steps including the finite element modeling, the model reduction, the derivation of the equations of motion, the establishment of a feedback control and the transient time simulation must be performed in each optimization loop. The optimization procedure along with the explanation of the floating frame of reference approach used in the modeling of the multibody system are discussed in section 2 and 3.

Such an optimization is applicable to efficiently design flexible multibody systems. However, important questions arise, concerning the robustness of the obtained system design. The design is optimized based on a nominal model. Here, it is analyzed how uncertainties in the optimization model might deteriorate the performance of the optimized system.

The application example of a flexible two-arm manipulator is used in this paper to study and illustrate the uncertainties in a multibody system. In the modeling and optimization, two important parameters are the choice of shape functions and the objective function. Differences in these choices will change the approximations made in the modeling and, thus, different results are expected. In the chosen application example, topology optimization is performed based on the desired output trajectory of the end-effector point, which is specified in time and space. The manipulator should track the predefined trajectory as closely as possible. It is therefore also discussed how changes of the desired output trajectory influences the system performance, i.e. the error of the end-effector trajectory. Another varying parameter is the payload of the manipulator. In section 4, it is discussed how the changes in these modeling choices will affect the performance of the multibody system.

2. Floating Frame of Reference Approach

In flexible multibody systems the bodies undergo large nonlinear rigid body motions and additionally show non-negligible deformations. Restricting the deformations to be small, as occurring in most typical machine dynamics and robotics applications, elastic bodies can be described efficiently using the floating frame of reference approach [9,10]. Thereby, the small deformation $\boldsymbol{u}$ of a flexible body is described in a body related reference frame K_R, which experiences large translational and rotational motion. The small elastic displacements are approximated using a global Ritz approach to separate the time- and position-dependent parts,

$$\boldsymbol{u}(\boldsymbol{R}_{RP}, t) \approx \boldsymbol{\Phi}(\boldsymbol{R}_{RP})\boldsymbol{q}_e(t). \tag{1}$$

Therein $\boldsymbol{q}_e$ are the elastic generalized coordinates. The matrix $\boldsymbol{\Phi}$ contains the shape functions and $\boldsymbol{R}_{RP}$ describes the position of a body-fixed point P in relation to K_R in reference configuration. For the rotations a similar Ritz-approach with the corresponding shape functions $\boldsymbol{\Psi}$ is used. The shape functions can be obtained, for instance, from a linear finite element model of the flexible body. However, since the inclusion of a complete finite element mesh in the flexible multibody system is computationally inefficient a linear model reduction of the finite element model is usually performed. Then, all necessary elastic data is evaluated and provided by standard input data (SID) files [11].

The equations of motion in minimal form are obtained by considering all constraints in the assembled system depending on generalized coordinates $\boldsymbol{q} = [\boldsymbol{q}_r^T,\ \boldsymbol{q}_e^T]^T \in \boldsymbol{R}^f$. Thereby, the vector of generalized coordinates contains the coordinates $\boldsymbol{q}_r \in \boldsymbol{R}^{f_r}$ representing the f_r degrees of freedom of the rigid body motion. The elastic coordinates $\boldsymbol{q}_e \in \boldsymbol{R}^{f_e}$ are the collection of the elastic generalized coordinates of all flexible bodies. The equations of motion in minimal coordinates read

$$\boldsymbol{M}(\boldsymbol{q})\ddot{\boldsymbol{q}} + \boldsymbol{k}(\boldsymbol{q}, \dot{\boldsymbol{q}}) + \widetilde{\boldsymbol{k}}(\boldsymbol{q}, \dot{\boldsymbol{q}}) = \boldsymbol{g}(\boldsymbol{q}, \dot{\boldsymbol{q}}) + \boldsymbol{B}(\boldsymbol{q})\boldsymbol{b}. \tag{2}$$

Here $\boldsymbol{M} \in \boldsymbol{R}^{f\times f}$ is the generalized mass matrix, $\boldsymbol{k} \in \boldsymbol{R}^f$ the vector of generalized Coriolis, gyroscopic and centrifugal forces, $\widetilde{\boldsymbol{k}}$ the vector of generalized inner forces, and $\boldsymbol{g} \in \boldsymbol{R}^f$ the vector of generalized applied forces. The input matrix $\boldsymbol{B} \in \boldsymbol{R}^{f\times m}$ distributes the control inputs $\boldsymbol{b} \in \boldsymbol{R}^m$ onto the directions of the generalized coordinates. For multibody

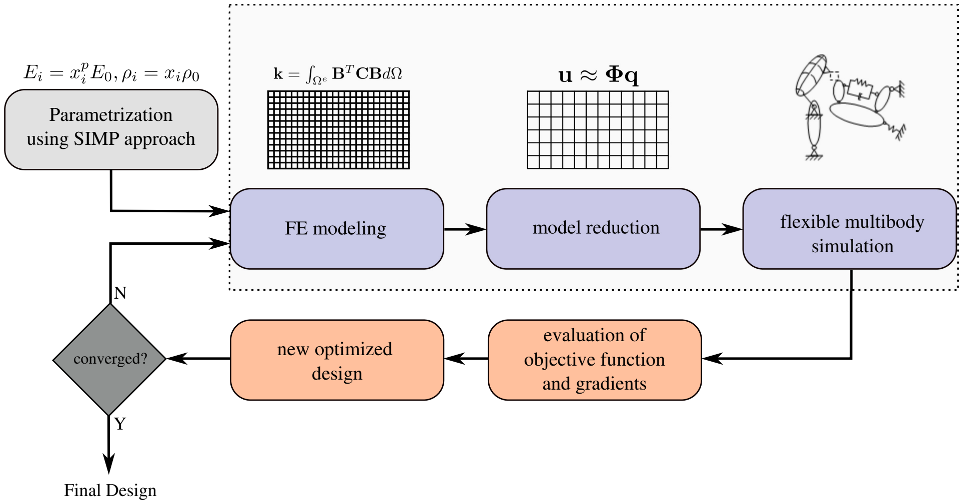

Fig. 1. Steps of the topology optimization loop for flexible multibody systems.

systems in chain or tree structure the equations of motion in minimal coordinates (2) are obtained in a straightforward way. For systems with kinematic loops one might use coordinate partitioning [12].

Following the distinction of the generalized coordinates into rigid coordinates $\boldsymbol{q}_r$ and elastic coordinates $\boldsymbol{q}_e$ the equations of motion can also be written as

$$\begin{bmatrix} \boldsymbol{M}_{rr} & \boldsymbol{M}_{re} \\ \boldsymbol{M}_{re}^T & \boldsymbol{M}_{ee} \end{bmatrix} \begin{bmatrix} \ddot{\boldsymbol{q}}_r \\ \ddot{\boldsymbol{q}}_e \end{bmatrix} + \begin{bmatrix} \boldsymbol{k}_r \\ \boldsymbol{k}_e \end{bmatrix} + \begin{bmatrix} \mathbf{0} \\ \boldsymbol{K}_{ee}\boldsymbol{q}_e + \boldsymbol{D}_{ee}\dot{\boldsymbol{q}}_e \end{bmatrix} = \begin{bmatrix} \boldsymbol{g}_r \\ \boldsymbol{g}_e \end{bmatrix} + \begin{bmatrix} \boldsymbol{B}_r \\ \boldsymbol{B}_e \end{bmatrix} \boldsymbol{b}. \tag{3}$$

Here $\boldsymbol{K}_{ee} \in \boldsymbol{R}^{f_e \times f_e}$ represents the structural stiffness matrix and $\boldsymbol{D}_{ee} \in \boldsymbol{R}^{f_e \times f_e}$ the structural damping matrix. It is noted, that in serial flexible manipulators the actuation occurs only at the joints. In this case, using relative coordinates and a tangent frame of reference for the elastic bodies, the control inputs $\boldsymbol{b}$ act directly on the rigid coordinates $\boldsymbol{q}_r$. This yields $\boldsymbol{B}_r = \boldsymbol{I}$ and $\boldsymbol{B}_e = \mathbf{0}$, where $\boldsymbol{I}$ is the identity matrix.

3. Optimization Procedure

Static topology optimizations of flexible bodies are often performed using finite element models. Thereby the objective functions are usually defined with respect to the compliance, displacements or stresses of the structure obtained from a set of static load cases. In contrast, in this paper the objective functions are computed from the results of fully dynamical simulations of the considered flexible multibody systems, whereby the relevant loads on the flexible members are captured.

The optimization loop for flexible multibody systems is much more complex than for static problems. The steps of the optimization loop are presented schematically in Fig. 1. Starting from an initial design, at first a finite element model of the flexible body is created. For the topology optimization the solid isotropic material with penalization (SIMP) approach is utilized. Then a model reduction of the parameterized finite element model is performed and the necessary SID files for the flexible bodies are calculated. Next, the equations of motion of the flexible multibody system are derived, a suitable control of the active system might be established and the time simulation is performed. Finally, the objective function as well as the constraint equations, if present, are evaluated from the time simulation results. Also the gradients of the criterion functions in respect to the design variables are computed. Objective function, constraint equations and gradients are then passed to the numerical optimization algorithm which subsequently suggests an improved design. Here the method of moving asymptotes [13] is used as optimization algorithm. With the improved design the optimization is repeated until a termination criterion is reached.

In this paper the optimization procedure is established using Matlab. The flexible multibody system is modeled using Neweul-M^2, which is a multibody simulation software able to derive the equations of motion for both rigid and flexible multibody systems [14]. For the reduction of the elastic degrees of freedom the Matlab based tool MatMorembs is used [15], which provides a variety of model reduction methods, e.g. modal truncation, component mode synthesis, reduction methods based on Krylov subspaces and model reduction methods based on Gramian matrices.

3.1. The SIMP Approach

In topology optimization of elastic bodies a limited amount of mass shall be distributed in a design domain such that an objective function, e.g. the compliance, is minimized under given loads. Therefore the design domain is discretized using finite element method. In topology optimization of such structures each finite element is one design subdomain and in the optimization it is desired that each subdomain is either empty or filled with material. A common method for relaxing this kind of mass/no-mass integer optimization problem is the SIMP approach. Thereby, continuous density-like design parameters $x_i \in (0, 1]$ are introduced for each subdomain as design variables. The design variables are gathered in the vector $\boldsymbol{x} \in R^m$. Following [16], the effective density and stiffness of one element are computed as

$$\rho_i = x_i \rho_0 \qquad \text{and} \qquad E_i = x_i^p E_0, \tag{4}$$

wherein ρ_0 and E_0 represent the density and the Young's modulus of the linear solid material. In order to enforce designs which possess only empty ($x_i = 0$) and filled ($x_i = 1$) elements the mass is penalized linearly whereas the stiffness is penalized using a power law with exponent p.

The basic penalization strategy (4) originates in static applications. However, it turns out that it is unsuitable for dynamical problems such as the fundamental eigenvalue maximization. In such applications localized modes are likely to arise in low density $x_i < 0.1$ areas [7]. These spurious modes originate from the excessive mass-to-stiffness penalization ratio for small values of x_i. Thus, for dynamical applications the SIMP laws must be adapted by changing the penalization strategy for small values of x_i. In the SIMP law proposed by Pedersen [7] the penalization of the stiffness is reduced. In the SIMP law by Olhoff and Du [6] the penalization of the mass is increased. A third SIMP law is proposed here which employs a two material interpolation SIMP scheme, where the stiffness and the density of the second material are very low [8]. Compared with the other two approaches this formulation results in continuously differentiable penalization laws for stiffness and density. This penalization can be formulated as

$$\rho_i = (\epsilon + x_i(1-\epsilon))\rho_0 \qquad \text{and} \qquad E_i = (\epsilon + x_i^p(1-\epsilon))E_0, \tag{5}$$

in which ϵ can be arbitrarily chosen as a small number.

3.2. Optimization Problem Formulation

In order to apply simple basic control strategies known from rigid multibody systems in active lightweight structures, it is required that the flexible structures behave, at least at their desired system output, similar to a rigid system. Thus, the tracking error

$$e(t) = ||\boldsymbol{r}_f(t) - \boldsymbol{r}_r(t)|| \tag{6}$$

is introduced. The position of the system output of the lightweight flexible system is denoted by $\boldsymbol{r}_f$ and the corresponding output of an ideal equivalent rigid system is denoted by $\boldsymbol{r}_r$. The latter is therefore the desired system output trajectory. Hence, in topology optimization a design is searched, which minimizes this tracking error $e(t)$. This is done here indirectly, by relating the tracking behavior to the deformation energy of the structure, i.e. the compliance of a single flexible body,

$$c(t) = \boldsymbol{u}^T(t)\boldsymbol{K}\boldsymbol{u}(t). \tag{7}$$

Therein $\boldsymbol{K}$ is the SIMP parameterized stiffness matrix of the unreduced finite element model and $\boldsymbol{u}(t)$ the corresponding nodal displacements.

In a strong formulation the compliance is considered in an integral form over the simulation time. However, the sensitivity analysis of such functional objective functions is highly cumbersome and computationally expensive, especially considering the large number of design variables. In order to circumvent the gradient computation of functional criteria, the equivalent static load method is employed. In this method a set of equivalent static loads is used, which is derived from the results of the time simulation of the flexible multibody system. Rearranging the lower part of the equations of motion (3) with respect to the stiffness of the elastic coordinates yields

$$\boldsymbol{K}_{ee}\boldsymbol{q}_e = -\boldsymbol{M}_{re}^T\ddot{\boldsymbol{q}}_r - \boldsymbol{M}_{ee}\ddot{\boldsymbol{q}}_e - \boldsymbol{k}_e - \boldsymbol{D}_{ee}\dot{\boldsymbol{q}}_e + \boldsymbol{g}_e + \boldsymbol{B}_e\boldsymbol{b} = \boldsymbol{f}_{eq}. \tag{8}$$

Herein $\boldsymbol{f}_{eq}$ represents the equivalent static load of all dynamic loads which are applied to the flexible bodies. Equation (8) has a similar structure as static topology optimization problems. However, the right-hand side, $\boldsymbol{f}_{eq}$, is not independent of the design variables. The trajectories of the elastic coordinates $\boldsymbol{q}_e$ are obtained by time simulation. Therefore, the equivalent static load $\boldsymbol{f}_{eq}$ does not have to be computed explicitly. Instead, with the elastic coordinates $\boldsymbol{q}_e(t_j)$ at a given time point t_j the nodal displacement field $\boldsymbol{u}_j$ of the unreduced structure is computed by Eq. (1) and the compliance computation follows then from Eq. (7).

In the optimization several equivalent static load cases can be considered. Here, the time domain is divided into n equal-sized intervals and in each interval the time t_j is identified at which the compliance or the tracking error becomes maximal. The overall optimization problem can then be formulated as

$$\begin{aligned} &\underset{\boldsymbol{x}\in\boldsymbol{R}^m}{\text{minimize}} \quad c(\boldsymbol{x}) \quad \text{with} \quad c = \sum_{j=1}^{n} \boldsymbol{u}_j^T \boldsymbol{K} \boldsymbol{u}_j \\ &\text{subject to} \quad h(\boldsymbol{x}) = -V_0 + \sum_{i=1}^{m} x_i \leq 0 \quad \text{and} \quad \underline{\boldsymbol{x}} \leq \boldsymbol{x} \leq \overline{\boldsymbol{x}}. \end{aligned} \tag{9}$$

Beside the minimization of the compliance c, a volume restriction h as well as the lower bound $\underline{\boldsymbol{x}}$ and upper bound $\overline{\boldsymbol{x}}$ for the design variables are defined.

An advantage of this procedure is that the gradient computation is eased dramatically compared to functional objective functions. Since the sensitivity information is computed with respect to the equivalent static loads, it can be calculated using an adjoint approach. For instance, employing the two material interpolation SIMP approach (5) the compliance is given as

$$c = \sum_{j=1}^{n}\sum_{i=1}^{m}(\epsilon + x_i^p(1-\epsilon))\boldsymbol{u}_j^{i\,\mathrm{T}}\boldsymbol{K}_0^i\boldsymbol{u}_j^i \tag{10}$$

with $\boldsymbol{K}_0^i$ represents the local stiffness matrix of element i with modulus E_0. In $\boldsymbol{u}_j^i$ the nodal displacements of element i from the load case j are provided. According to this parametrization and assuming the equivalent static load vector $\boldsymbol{f}_{eq}$ to be constant the sensitivities are computed as

$$\frac{\partial c}{\partial x_i} = -p(1-\epsilon)x_i^{p-1}\sum_{j=1}^{n}\boldsymbol{u}_j^{i\,\mathrm{T}}\boldsymbol{K}_0^i\boldsymbol{u}_j^i, \quad i = 1, ..., m. \tag{11}$$

However, assuming $\boldsymbol{f}_{eq}$ to be design independent is a severe simplification in dynamic applications, compare Eq. (8). Indeed, the dynamic loads are dependent on the design variables which are the density ratios of the finite elements. Thus, on the one hand, the assumption of design independent loading eases the gradient computation significantly. On the other hand, it is not any more the exact gradient of the dynamical problem. In many cases, this does not hinder the convergence of the optimization procedure to a better performing design. Nevertheless, for specific cases where the loading originates dominantly from the inertia forces of the optimized bodies, the calculation of exact gradients are shown to be necessary [18].

4. Optimization Results and Uncertainty Investigation

The example of a flexible manipulator shown in Fig. 2 is used to demonstrate the implementation of the previously discussed methods and to investigate the robustness of the modeling and optimization with respect to uncertain parameters in the model.

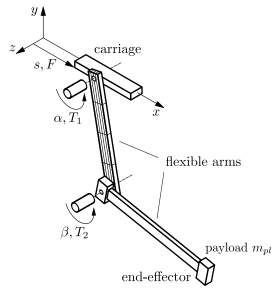

Fig. 2. Benchmark example: two-arm manipulator.

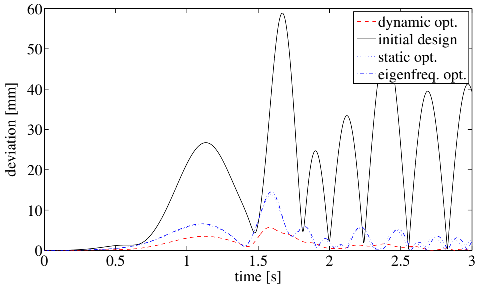

Fig. 3. End-effector deviation of the manipulator for the initial design and the optimized design using different objective functions

The flexible manipulator consists of a rigid cart and two arms and possesses $f_r = 3$ rigid-body degrees of freedom. The system inputs are the forces and torques, which act at the joints and the system output is the end-effector point. The forces and torques are chosen such that the rigid coordinates $\boldsymbol{q}_r$ follow exactly the trajectories which are necessary that the end-effector of an equivalent rigid system follows a predefined semi-circular path. For the two flexible arms it is assumed that they are made out of aluminum and have initial dimension $(1.00 \times 0.06 \times 0.01)$ m.

4.1. Model Uncertainty

In the modeling and simulation of a system, it is decisive to know how the real world structure should be approximated. Hence, a class of uncertainties is introduced which roots in the approximations and simplifications made on the model. These approximations could result in an underestimation or overestimation of certain parameters in the system. This error will consequently propagate in the model and the outputs of the simulation will be also uncertain. The intensity of uncertainty in the output depends on how strong or weak the relation between an uncertain model parameter and a model output is. Here, in order to investigate different aspects of model uncertainty in the two-arm manipulator, the choices of objective function as well as different model reduction techniques and reduced model size are addressed.

The main optimization is formulated as minimal compliance problem, in which the loads are computed from the flexible multibody simulation. In section 3 it is explained, how the dynamic loads in a discretized time domain are captured using the equivalent static load method. However, it is also possible to select other objective functions for the optimization. Two alternatives are the fundamental eigenfrequency of the structure or the compliance of the structure under static displacement fields. Both possibilities are computationally very efficient since they do not consider the dynamic loads. In these cases, the optimization is isolated from the multibody system simulation. Here, using the first alternative objective function, the optimization problem formulation is changed to the maximization of the fundamental eigenfrequency. For the second alternative objective function, the compliance is calculated similar to (7), with the difference that static unit loads are considered in the computation of the deformations. In Fig. 3, the end-effector deviation of the designs, which are optimized with these two alternative objective functions are shown along with the initial design and the optimized design considering the dynamic loads. Even though by the static and eigenfrequency optimization, the maximum deviation is decreased to about one fourth, it is yet considerably higher in comparison to the design obtained using the presented dynamical optimization procedure. The optimized structures using these different objectives are shown in Fig. 4.

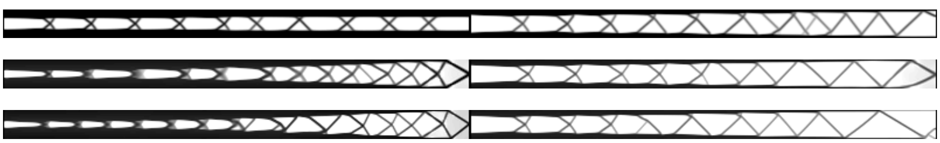

Fig. 4. Optimized design with dynamic loads (top), static compliance (middle) and eigenfrequency (bottom)

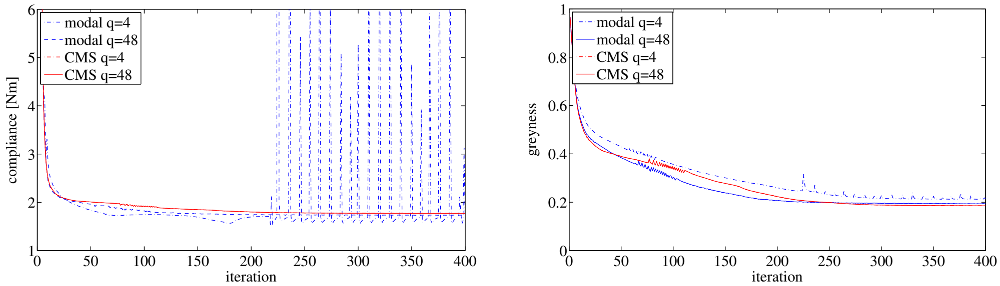

Fig. 5. Convergence of compliance (left) and grayness (right) by using modal truncation and CMS

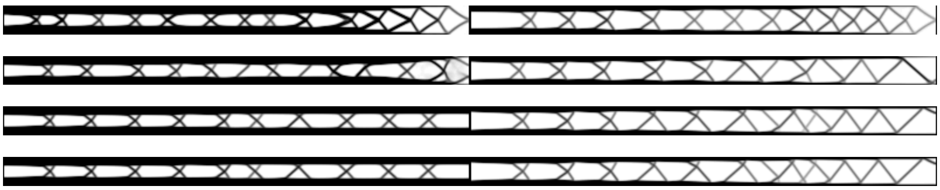

Fig. 6. Optimized design using (top to bottom) modal truncation with $q = 4$ and $q = 48$, CMS with $q = 4$ and $q = 48$

In the modeling and optimization of flexible multibody systems, the choice of shape functions are shown to be of great importance [19]. Therefore, two model reduction methods namely modal truncation and component mode synthesis (CMS) [22,23] are examined in this context. Since the deformation of the flexible parts are approximated by a set of shape functions which are computed in the model reduction procedure, see Eq. (1), it is crucial to have a set of shape functions which are capable of capturing the dominating deformations in the flexible bodies.

Modal truncation is a well known and widely used method in many applications. By applying this model reduction method, the deformation of flexible parts are approximated by a selection of eigenvectors of that body. In the CMS method, elastic deformations are approximated by a set of eigenvectors and constraint modes. Constraint modes are shape functions that result from the static deformation of the structure when a unit displacement is applied to each interface coordinate while the other interface coordinates are fixed [23].

Using the two aforementioned model reduction methods the optimization convergence behavior is analyzed in Fig. 5. Thereby, the compliance, which is the objective function, and the grayness are plotted. The grayness is a measure of number of gray elements, which are neither full nor empty [20]. It is computed from the values of the design variables as

$$g = 4/m \sum_{i=1}^{m} x_i(1 - x_i) \tag{12}$$

where m is the number of elements. For $g = 1$, all elements have intermediate density, whereas $g = 0$ indicates the convergence of all element density ratios to either 0 or 1. It is seen that the compliance converges faster than the grayness. However, as shown in Fig. 5 the convergence behavior of the compliance is unacceptable when modal truncation with low number of modes, i.e. four modes per arm, is used. By increasing the number of modes, convergence behavior for the case of modal truncation will be similar to that of the CMS reduction. Qualitative inspection of the optimized structures which are illustrated in Fig. 6 shows that using CMS method, the topology of the optimized structure is not distinctively influenced by the number of modes selected for the approximation of the deformations. Also a similar design is obtained using modal truncation with large number of modes. On the other hand, the convergence of grayness is similar for both model reduction methods and for different number of modes.

In order to investigate the model reduction in more detail, the initial design and one optimized design are simulated using modal truncation and CMS with varying number of modes. The value of the compliance is not influenced by the changes in the number of modes when CMS is used. This is in strong contrast to the case when modal truncation is used. In Fig. 7 it is shown how increasing the number of mode shapes for a single structure affects the estimated

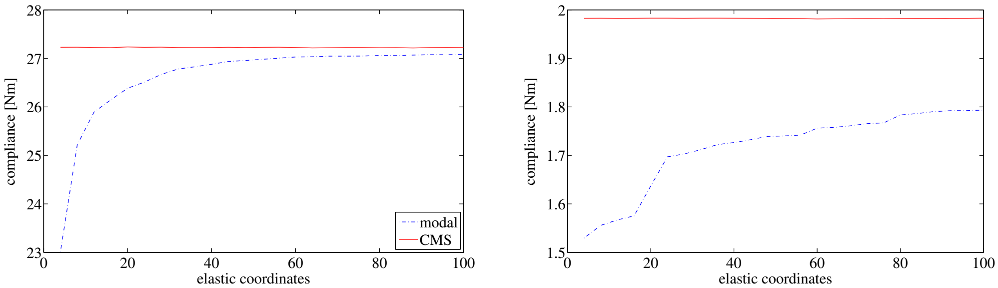

Fig. 7. Compliance of initial design (left) and the final design (right) for different number of modes.

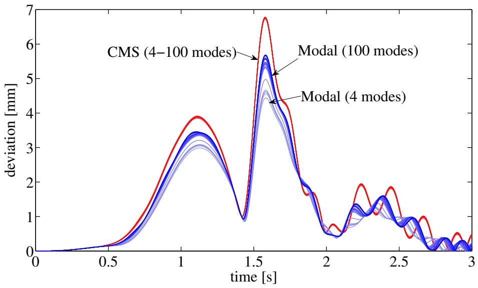

Fig. 8. End-effector deviation of an optimized structure simulated with modal truncation and CMS

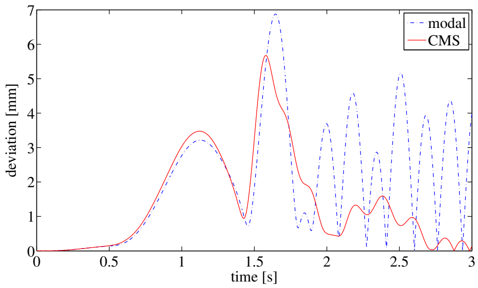

Fig. 9. End-effector deviation of optimized structure with modal truncation and CMS

compliance and the end-effector deviation. With lower number of modes in modal truncation, it is not possible to capture all the deformations, hence, the stiffness of the structure is overestimated. The value of the compliance using modal truncation reaches that of CMS method by increasing the number of modes for the simple initial design where all the elements are equally set to half density. For the more complex optimized design, the stiffness of the structure is overestimated even when the number of modes is increased in the modal truncation. The same behavior is illustrated in Fig. 8 which shows the end-effector deviation over the time domain. Here, one optimized structure is simulated with modal truncation and CMS. Thereby, the estimated end-effector deviation increases by increasing the number of modes when the modal truncation is used.

The previous discussion shows that it is clearly advantageous to use CMS compared to modal truncation. Thus, a more exact approximation of the deformations of the elastic bodies is obtained. In order to investigate the performance gain using CMS method, two structures optimized with modal truncation and CMS, respectively, are simulated with CMS. The result of this comparison is plotted in Fig. 9. The choice of model reduction method in the optimization leads to 14% difference comparing the maximal end-effector deviations in this example, showing that the use of CMS method in the optimization is more favorable. However, this difference is smaller compared to the difference resulting by the choice of objective function. Thus, the improvement in the performance is in some respects independent of the model reduction method.

4.2. Application Uncertainty

A separate class of uncertainties is related to application uncertainty which is the changes that might occur in the parameters of a system corresponding to its operation. With the problem formulation in Eq. (9), the system is optimized using one specific application setup with crisp-valued parameters. In the presented application example, flexible arms are optimized for a predefined trajectory and payload. In this example, the application uncertainty can be interpreted as the changes in the payload of the manipulator as well as changes in the trajectory of the end-effector.

It is rather foreseeable how changes in the end-effector payload would affect the performance of the system. In order to quantitatively illustrate this dependency, the payload m_{pl} is varied from 4 to 8 kg where the nominal value used in the optimization is $m_{pl} = 6$ kg. The changes in the compliance and in the maximum end-effector deviation

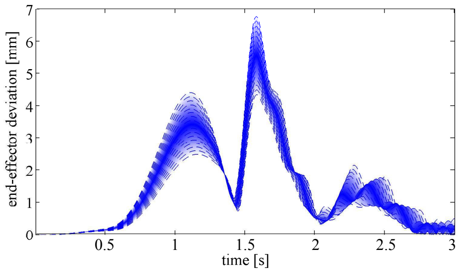

Fig. 10. End-effector deviation of the manipulator for different payloads m_{pl} from 4 to 8 kg.

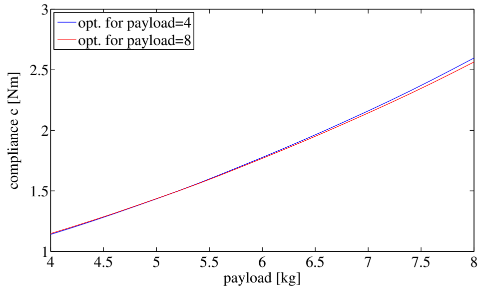

Fig. 11. Compliance for two optimized designs with different payloads m_{pl} = 4 kg and m_{pl} = 8 kg.

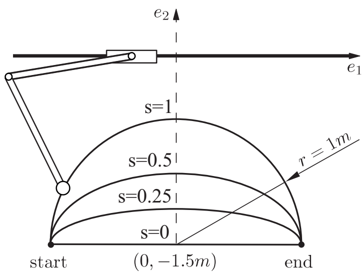

Fig. 12. Change in the trajectory of the manipulator.

is as expected nearly linear. This is shown in Fig. 10 where the desaturation of color corresponds to the amount of deviation from the nominal payload.

Fig. 11 shows how using one structure for different payloads affects the performance of the system. In this case, two structures that are respectively optimized for the payloads of 4 kg and 8 kg, are simulated for different values of payload. Here, the maximum error between the two designs is only 1.2%. In a practical application, the obtained optimized design which is used in this application example is considered insensitive to changes in the payload.

In the last study, the trajectory of the manipulator is chosen as the uncertain parameter. In the optimization setup of the system, the desired end-effector trajectory is a semi-circular path. For testing purpose, in the model with uncertainty, the trajectory varies from the semi-circle to a straight line. Changes in the trajectory are shown in Fig. 12 where every path is characterized by the value $s \in [0, 1]$. Parameter s is the ratio of maximum change in vertical direction to the initial radius of the circular path $r = 1$ m. Thus, $s = 1$ and $s = 0$ designate a semi-circular path and a straight line, respectively.

Plots of the end-effector deviation in Fig. 13 illustrate the changes in deviation as the trajectory of the manipulator is altered. These results show changes in the value of deviation and also changes in the time point at which the deviation

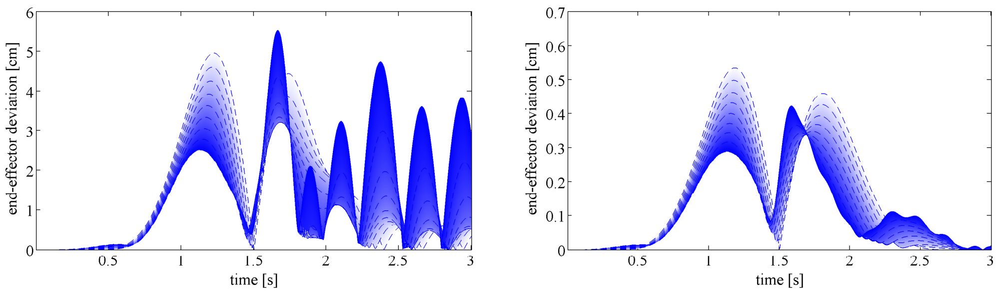

Fig. 13. End-effector deviation for the initial design (left) and optimized design (right) for different trajectories.

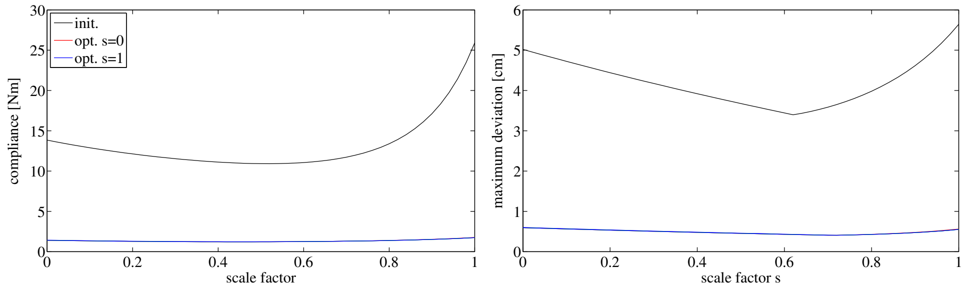

Fig. 14. Compliance (left) and maximum end-effector deviation (right) of initial and optimized design for different trajectories.

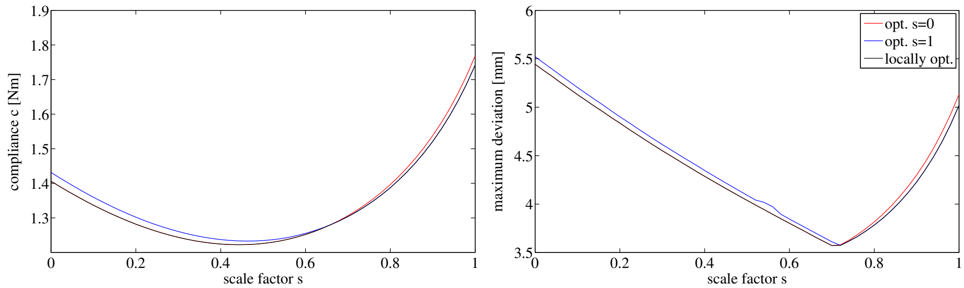

Fig. 15. Compliance (left) and maximum end-effector deviation (right) of optimized design for different trajectories.

for the initial design and the optimized design becomes maximal. Regardless of the trajectory, the optimized design yields tracking errors which are less than a tenth of the initial design.

In Fig. 14, the value of compliance and the maximum end-effector deviation of the optimized structure and the initial design are plotted for the different trajectories where optimization have been performed for $s = 0$ and $s = 1$. It shows how the applied dynamic load on the flexible arms and the value of compliance and the maximum end-effector deviation changes as s is varied from 0 to 1. For the initial design, the maximum change in compliance is 57% while it is 28% for the optimized structure. Thus, the optimized structure is more robust against changes in the trajectory compared to the initial design.

Moreover, it is important to measure the changes imposed on the compliance and end-effector deviation if a structure which is optimized for one specific trajectory is used for a different trajectory. On that account, the compliance and maximum deviation for two structures with different trajectories in the optimization are plotted in Fig. 15. At any different scale factor s, the performance of the structure which is optimized specifically for that trajectory is better compared to the other structures. However, the maximum error is 1.8% for compliance and 2.2% for maximum deviation. In other words, if one structure is optimized for a specific trajectory and used for other trajectories defined by $s \in [0, 1]$, it leads to no more than 1.8% increase in the compliance compared to the structure which is optimized specifically for that trajectory. Thus, for this application example the design is robust to changes in the desired end-effector trajectories.

5. Conclusion

In this paper a topology optimization procedure for optimal design of flexible multibody systems using the floating frame of reference approach is analyzed. The optimization is based on fully dynamical simulations and equivalent static loads. In this framework, the robustness of the optimized design is investigated by considering different classes of uncertainties which might arise in the system, i.e. the model uncertainty and the application uncertainty. For this purpose, a series of topology optimizations has been performed for a flexible two-arm manipulator. It is shown that the optimized flexible structure obtained from the optimization procedure is robust in the case that application uncertainties are introduced in the system. Furthermore, the effect of uncertainties in the modeling and optimization of the structure is shown to be more pronounced. In particular, the choice of the objective function is crucial to the performance of the optimized structure and shows the need for including the actual dynamic loads. Moreover, in the model reduction, the choice of CMS is clearly advantageous to modal truncation and results in non-negligible performance gain in the presented application example. The obtained design is robust against application uncertainties such as change of end-effector trajectories and shows predictable behavior for uncertainties in the end-effector mass.

References

1. Albers, A., Ottnad, J., Weiler, H., Haeussler, P.: Methods for Lightweight Design of Mechanical Components in Humanoid Robots. IEEE-RAS International Conference on Humanoid Robots, Pittsburg, Pennsylvania, USA, 2007.
2. Brüls, O., Lemaire, E., Duysinx, P., Eberhard, P.: Optimization of Multibody Systems and their Structural Components. Multibody Dynamics: Computational Methods and Applications, K. Arczewski, W. Blajer, J. Fraczek, M. Wojtyra (Eds.), Computational Methods in Applied Sciences, Vol. 23, Springer, pp. 49-68 , 2011.
3. Held, A.; Seifried, R.: Topology Optimization of Members of Elastic Multibody Systems. PAMM Proceedings in Applied Mathematics and Mechanics, Vol. 12, pp. 67-68, 2012.
4. Seifried, R.: Dynamics of Underactuated Multibody Systems - Modeling, Control and Optimal Design, Solid Mechanics and Its Applications, Vol. 205, Springer, 2014.
5. Seifried, R.; Held, A.: Optimal Design of Lightweight Machines using Flexible Multibody System Dynamics. Proceedings of the ASME 2012 International Design Engineering Technical Conferences (IDETC/CIE 2012), August 12-15, 2012, Chicago, IL, USA, paper ID DETC2012-70972.
6. Olhoff, N., Du, J.: Topological Design of Continuum Structures Subjected to Forced Vibration. In 6th World Congresses of Structural and Multidisciplinary Optimization, 2005.
7. Pedersen, N.: Maximization of Eigenvalues using Topology Optimization. Structural and Multidisciplinary Optimization, Vol. 20, pp. 2–11, 2000.
8. Moghadasi, A.: Modeling and Analyzing the Influence of Bearing Loads in the Topology Optimization of Flexible Multibody Systems, Master's thesis. Institute of Engineering and Computational Mechanics, University of Stuttgart, 2013.
9. Schwertassek, R., Wallrapp, O.: Dynamik flexibler Mehrkörpersysteme (in German). Braunschweig: Vieweg, 1999.
10. Shabana, A.A.: Dynamics of Multibody Systems. New York: Cambridge University Press, 3. Edn., 2005.
11. Wallrapp, O.: Standardization of Flexible Body Modeling in Multibody System Codes, Part 1: Definition of Standard Input Data. Mechanics of Structures & Machines, Vol. 22, No. 3, pp. 283–304, 1994.
12. Wehage, R.A., Haug, E.J.: Generalized Coordinate Partitioning for Dimension Reduction in Analysis of Constrained Dynamical Systems. Journal of Mechanical Design, Vol. 104, pp. 247–255, 1982.
13. Svanberg, K.: The Method of Moving Asymptotes - A New Method for Structural Optimization. International Journal for Numerical Methods in Engineering, Vol. 24, pp. 359–373, 1987.
14. Kurz, T., Eberhard, P., Henninger, C., Schiehlen, W.: From Neweul to Neweul-M^2: Symbolical Equations of Motion for Multibody System Analysis and Synthesis. Multibody System Dynamics, Vol. 24, pp. 25-41, 2010.
15. Nowakowski, C., Fehr, J., Fischer, M., Eberhard, P.: Model Order Reduction in Elastic Multibody Systems using the Floating Frame of Reference Formulation. In Proceedings MATHMOD 2012 - 7th Vienna International Conference on Mathematical Modelling, Vienna, Austria, 2012.
16. Bendsoe, M., Sigmund, O.: Topology Optimization - Theory Methods and Applications. Berlin: Springer, 2003.
17. Kang, B., Park, G.: Optimization of Flexible Multibody Dynamic Systems Using the Equivalent Static Load Method. AIAA Journal, Vol. 43, pp. 846-852, 2005.
18. Held, A.: On Structural Optimization of Flexible Multibody Systems. PhD Thesis, University of Stuttgart: Stuttgart, 2014.
19. Held, A., Nowakowski, C., Moghadasi, A., Seifried, R., Eberhard, P.: On the Choice of Shape Functions in Topology Optimization of Flexible Multibody Systems. Structural and Multidisciplinary Optimization, submitted, 2014.
20. Sigmund, O.: Morphology-based Black and White Filters for Topology Optimization. Structural and Multidisciplinary Optimization, Vol. 33, pp. 401-424, 2007.
21. Seifried, R., Held, A., Moghadasi, A.: Topology Optimization of Members of Flexible Multibody Systems using the Floating Frame of Reference Approach. International Conference on Multibody System Dynamics, Busan, Korea, 2014.
22. Hurty, W.C.: Dynamic Analysis of Structural Systems using Component Modes. AIAA Journal 3, 678685, 1965.
23. Craig, R., Bampton, M.: Coupling of Substructures for Dynamic Analyses. AIAA Journal 6(7), 13131319, 1968.